PAPERS

Use of computed tomography in the diseased feline thorax

Computed tomography (CT) scanning of the thorax is gaining more attention in veterinary medicine as therapeutic possibilities increase. Plain and contrast-enhanced CT images of the thorax of five referred cats with signs of respiratory disease were evaluated using soft tissue (pleural) and lung windows. The common CT pattern in all cats was involvement of the lung lobes, either as a homogeneous or heterogeneous single lobe hyperdensity. It involved the main bronchus, invaded the cranial or caudal mediastinum, and crossed the border to the opposite lung. Right lung atelectasis and mediastinal shift caused left lung overinflation. Bronchial lymph node enlargement was found unilaterally or bilaterally. CT-guided percutaneous fine needle aspiration biopsy of the lobar lung lesion was performed in four cats; in three cases it revealed carcinoma and in one inflammation, although the cat with suspected inflammation was subsequently found to have a carcinoma on lung lobectomy. Histopathology confirmed lung metastasis in one case and bronchial adenocarcinoma in four cases. A protocol for systematic examination of thoracic CT images is proposed.

W. Henninger

Journal of Small Animal Practice (2003) **44**, 56–64

Radiology Clinic, University of Veterinary Medicine Vienna, A-1210 Vienna, Veterinärplatz 1, Austria

INTRODUCTION

Computed tomography (CT) has gained wide acceptance in veterinary medicine as a specialised imaging method, a useful preoperative technique and a precise staging tool (Ahlberg and others 1989, Burk 1991, Chen and others 1992, Delisle 1993, Hathcock and Stickle 1993, Henninger 1997, Henninger and Pavlicek 2001). In small animal medicine all parts of the body may be examined. In the literature, the reported frequency of the use of CT for thoracic imaging is lower than for imaging of the brain or spine. The thorax may be easily examined radiographically (Farrow and others 1994), but mediastinal structures are superimposed on radiographs; in particular, the cranial part of the mediastinum is not individually identifiable (Suter 1984, Thrall 1994). Reports of CT-based anatomy (Zook and others 1989, Assheuer and Sager 1997, Samii and others 1998, Henninger and Gutmannsbauer 1999) make interpretation of thoracic scans more easy, thus providing increased diagnostic information and allowing more specific therapy (Burk 1991, Tidwell and Johnson 1994, Henninger 1997, Schwarz and Tidwell 1999).

The aim of the present study is to describe the CT appearance of normal and abnormal thoracic structures in the cat, with particular emphasis on the mediastinal structures and lung pattern of selected clinical cases. The clinical and/or pathological outcome is compared to the typical CT appearance of each disease, and additionally the use of Hounsfield units (HU) and the value of CT-based percutaneous fine needle aspiration biopsy are documented.

MATERIALS AND METHODS

Four domestic shorthaired cats and one Persian cat with a history of respiratory signs were referred for CT examination of the thorax. A thorough physical examination, blood chemistry and thoracic radiographs were performed for each cat (Table 1). For CT examination, the animals had to be fasted for one day and in a condition to allow general anaesthesia. All cats, except cat 2, were sedated with a combination of 0·8 mg/kg midazolam (Dormicum; Roche), 0·4 mg/kg butorphanol (Butomidor; Richter) and 2 mg/kg ketamine (Ketalar; Parke-Davis) intravenously. For induction of anaesthesia, 3 to 5 mg/kg propofol (Diprivan; AstraZeneca) was administered intravenously. Anaesthesia was maintained after intubation with a mixture of isoflurane and oxygen. Rapidly breathing patients were ventilated after administration of a peripheral muscle relaxant intravenously (0·6 mg/kg rocuronium,Esmeron; Organon Teknika). The cats were monitored during the entire procedure. Four cats were positioned in sternal recumbency on the CT table. Cat 2 had been euthanased at the request of the owner before scanning, and was scanned in the supine position.

Table 1. Clinical, imaging, cytological and histopathological findings in five cats with thoracic disease

Cat	Breed	Sex	Age (yrs)	Body weight (kg)	History	Radiography	Thoracic CT-patterns*	CT-guided FNAB and cytology	Outcome
1	DSH	MN	8	4·0	Chronic dyspnoea, resistant to therapy	Dilated trachea, cavitary right caudal lobe mass	'Hepatic' appearance of right middle lobe (HU +37 to +45; *+70* to *+90*), bronchiectasis, bilateral bronchial lymph node enlargement (HU +51; *+89*)	Inflammation	Euthanased after right middle lobectomy; bronchial adenocarcinoma diagnosed postmortem
2	Persian	F	9	4·5	Acute dyspnoea	Right paramediastinal mass	Postmortem CT: solid mass around right main stem bronchus, associated mediastinal infiltration (HU +54 to +59), bilateral bronchial lymph node enlargement (HU +64)	—	Euthanased; bronchial adenocarcinoma of right caudal lung lobe diagnosed postmortem
3	DSH	MN	11	5·6	Progressive dyspnoea	Increasing opacity of the right lung lobes within three weeks, mediastinal shift	Bronchial obstructing mass (HU +48 to +64; *+97* to *+120*) led to total atelectasis of the right lung (HU +21 to +44; *+102* to *+116*), mediastinal shift, left lung emphysema (HU –884 to –889; *–861* to *–869*), right bronchial lymph node enlargement (HU +55; *+103*)	Bronchial carcinoma	Euthanased; bronchial adenocarcinoma of right middle lobe causing atelectasis of whole right lung. No postmortem examination
4	DSH	MN	11	7·5	Acute dyspnoea after abdominal surgery	Pleural effusion, right paramediastinal mass	Heterogeneous solid mediastinal mass (HU +36 to +44; *+ 56 to +97*) affecting the right caudal lung lobe and accessory lobe, pleural effusion (HU +2 to +5; *no enhancement*), enhancement of pleura (HU *+49* to *+57*), bilateral bronchial lymph node enlargement (HU +20; *+64*)	Pulmonary carcinoma	Euthanased after failed doxorubicin treatment; metastasis of colonic carcinoma diagnosed postmortem
5	DSH	FN	7·5	4·3	Slight dyspnoea, hindlimb lameness, swollen toes	Left paramediastinal mass; lucencies of the distal phalanges, periostitis, soft tissue swelling	Heterogeneous solid mass affecting the left caudodorsal lung lobe (HU +50 to +72; *+60* to *107*), peribronchial enhancement of fading dorsal subsegment bronchus (HU +70; *+176*); bilateral bronchial lymph node enlargement (HU +51; *+114*)	Bronchial carcinoma	Euthanased; bronchial adenocarcinoma of left caudal lung lobe and phalangeal metastases diagnosed postmortem

*Hounsfield units (HU) are given in parentheses; italicisation indicates after contrast enhancement
CT Computed tomography, DSH Domestic shorthaired, FNAB Fine needle aspiration biopsy, F Female, FN Neutered female, MN Neutered male

Initially, plain scans of either the whole thorax or of the cranial or caudal part of the thorax including the heart, were obtained, depending on the cat's clinical condition. Slice thickness was 2 mm or 5 mm, and the slice interval was preset at 2, 3 or 5 mm, respectively. The plain images were briefly viewed on the screen. Each plain examination, except for cat 2, was followed by the intravenous administration of 1·5 to 2·5 ml/kg of iodine contrast medium. Iopamidol (Jopamiro 300; Gerot) was administered at a flow rate of 0·2 to 0·3 ml/second using an automatic injection pump and the sequence was repeated immediately. All images were displayed in the soft tissue (so-called pleural) window (window level WL+40, window width WW750) and the lung window (WL-500, WW1500), and were printed on laser multiformat films (3M Dry View; Imation-Kodak). For further evaluation and follow-up studies, all series were stored digitally on CD-ROMs.

All anatomical structures were subsequently examined on the CT images using a protocol corresponding to the way in which thoracic radiographs are read. This started with the spine, ribs, sternum, surrounding musculature and fatty tissue. Next the pleural space and local changes adjacent to soft tissue opacities of the lung were examined. Within the long mediastinal area, the trachea and oesophagus were evaluated first, followed by hilar lymph nodes and main vessels, and then the heart. Finally, the right and left lungs were looked at and typical patterns of opacities, space occupying lesions, and bony and/or soft tissue infiltrations were described. Measurements of HU completed the description of the plain and contrast-enhanced pathologies.

CT-guided fine needle aspiration biopsies were taken after precise localisation of the lesion in four cats, and succesful puncture was documented by an immediate follow-up CT image. Cytological and clinical outcomes were noted and compared with the results of the CT examinations.

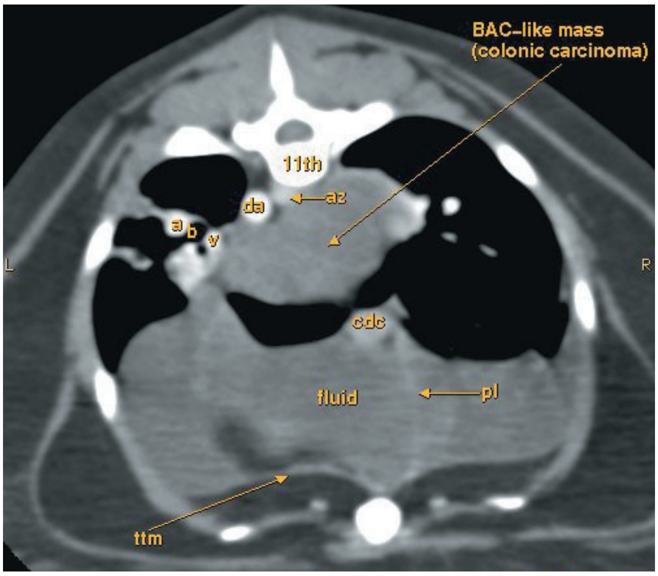

FIG 1. Contrast-enhanced CT scan of a feline thorax at the level of the 11th thoracic vertebra (cat 4); pleural window, sternal recumbency. The suspected bronchial adenocarcinoma affects the right caudal lung lobe and the caudodorsal mediastinum, displacing the right azygos vein and the descending aorta. Both caudal lung lobes are reduced in size, pleural effusion is present, and pleurae appear as perpendicular hyperdense lines within the fluid. The mass was identified as colonic metastasis histopathologically. 11th = 11th thoracic vertebra, da = Descending aorta, az = Right azygos vein, abv = Lobar artery, bronchus and vein of the left caudal lung lobe, BAC mass = metastasis of colonic carcinoma, cdc = Caudal vena cava, pl = Pleura, fluid = Free fluid within the pleural space, ttm = Transverse thoracic muscle

RESULTS

Spine, ribs, sternum and thoracic wall

Each thoracic vertebra appeared hyperdense, with a rather small body and a comparatively big arch encircling the isodense spinal cord, which was surrounded by a small rim of fatty tissue. Cat 2 showed ventral spondylosis and spondyloarthropathy at thoracic vertebra 10-11, but all of the other thoracic vertebrae were unremarkable.

The ribs, as bony structures, appeared hyperdense. The costospinal, costochondral and costosternal articulations were readily visualised. The cartilaginous rib arch was calcified in each cat. The sternum appeared as hyperdense quadrate, or sometimes rounded, bony sections.

In each cat, a great deal of subcutaneous, subfascial and intermuscular fat was present and allowed excellent differentiation of the musculature. Isodense sections surrounded the spine, showing soft tissue layers parallel to the ribs and extrathoracic pectoral muscles ventrally. In the ventral thoracic cavity, a bilaterally visible, thin soft tissue layer corresponding to the transverse thoracic muscle was easily identified extending to the xiphoid process, covering the internal thoracic artery and vein.

Pleural space and diaphragm

Parietal and visceral pleura were not visible in unaffected areas and merged with the inner thoracic wall, diaphragm and lungs, forming a smooth surface. In cases of diseased lung tissue, parietal and/or visceral pleura were thickened, irregularly defined (cats 1, 2 and 3) and showed enhancement after intravenous contrast injection. The pleural space itself was not visible, except

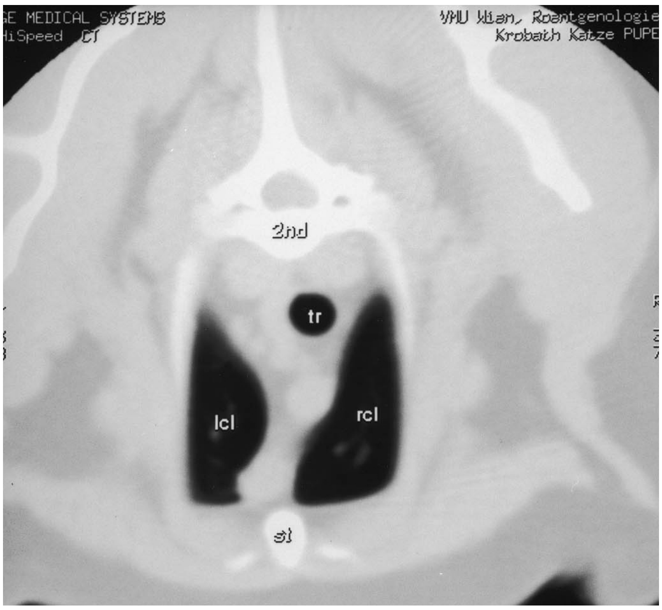

FIG 2. Contrast-enhanced CT scan of a feline thorax at the level of the second thoracic vertebra (cat 5); lung window, sternal recumbency. The left and right cranial lung lobes appear asymmetric to the right which is normal at this level. The mediastinum contains trachea, contrast-enhanced vessels and sternal lymph nodes. 2nd = Second thoracic vertebra, tr = Trachea, lcl = Left cranial lung lobe, rcl = Right cranial lung lobe, st = Sternum

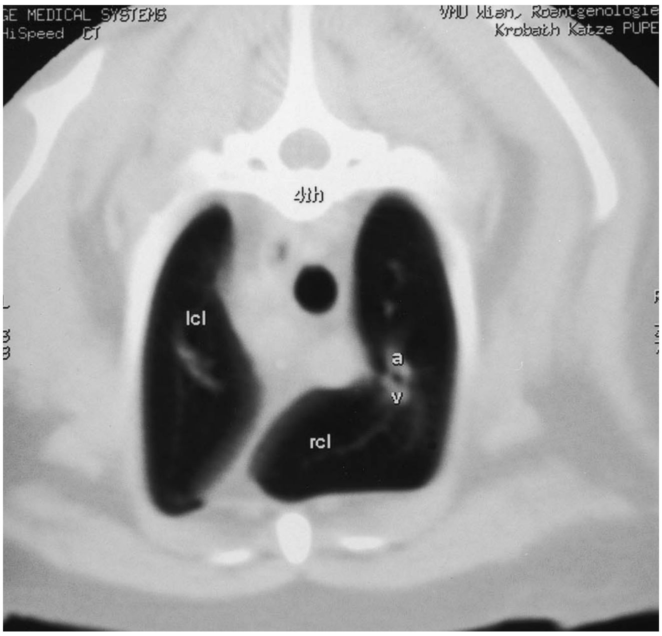

FIG 3. Contrast-enhanced CT scan of a feline thorax at the level of the fourth thoracic vertebra (cat 5); lung window, sternal recumbency. The tip of the right cranial lung lobe extends to the left and covers the heart; the lobar artery runs dorsal to the bronchus and the lobar vein ventral to it. 4th = Fourth thoracic vertebra, lcl = Left cranial lung lobe, rcl = Right cranial lung lobe, a = Lobar artery, v = Lobar vein

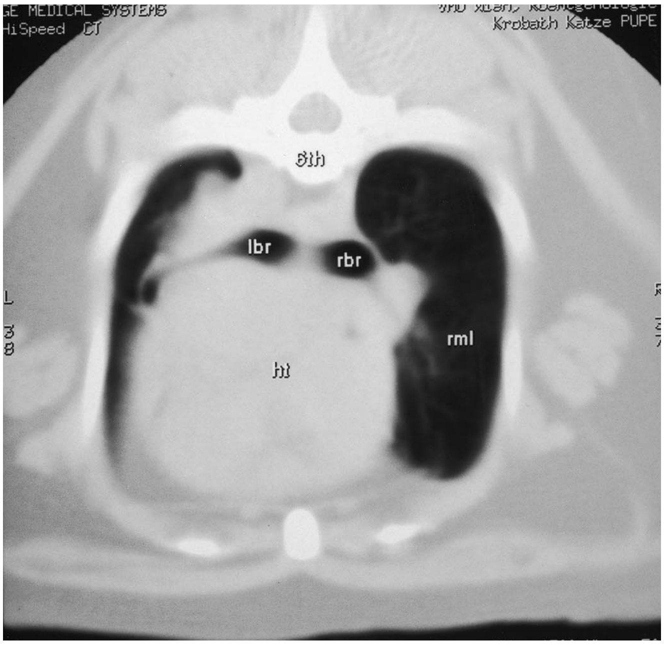

FIG 4. Contrast-enhanced CT scan of a feline thorax at the level of the sixth thoracic vertebra (cat 5); lung window, sternal recumbency. The left and right main stem bronchi originate at this level and the heart is enlarged and occupies nearly two-thirds of the thoracic space. The right middle lobe is larger than the caudal part of the left cranial lung lobe. 6th = Sixth thoracic vertebra, lbr = Left main stem bronchus, rbr = Right main stem bronchus, rml = Right middle lobe, ht = Heart

in cat 4 where a severe pleural effusion was present. The pleural walls, which were enhanced after intravenous contrast administration, formed septa within the accumulated fluid. Pleural fluid was not enhanced, and measured about 2 to 5 HU, corresponding to transudate.

Most of the diaphragm was not visible on the thoracic CT images, except the muscular left and right cura at the caudodorsal part of the thorax. The diaphragmatic cupula merged with the liver; the latter was consistently seen at the level of the caudal lung lobes. In the case of pleural effusion (cat 4), the diaphragm also remained invisible.

Mediastinum – trachea and oesophagus

The trachea was consistently seen in sections from the thoracic inlet to the bifurcation, and was used as a landmark. The normal tracheal diameter was 5 to 7 mm, and was not influenced by the respiratory phases. An increased tracheal lumen caused by chronic bronchial obstruction was seen in two cats – up to 9 mm in cat 3 and more severely up to 13 mm in cat 1; in the latter case, the distended trachea had previously been seen on the radiographs. On postmortem CT in cat 2, the lumen of the trachea was reduced to 3·5 mm and a dorsal notch indicated relaxation of the tracheal muscle. Displacement of the trachea to the right due to right lung collapse (in cat 3) was readily visible.

The oesophagus was also used as a landmark which could be followed easily through the whole thoracic cavity. It appeared slightly dilated and air-filled because of partial relaxation due to anaesthesia; its slit-like to rounded sections were about a quarter of the trachea's size. In cases of mass effects (cats 1, 2, 4 and 5) or mediastinal shift (cat 3), compression of the oesophagus led to its incomplete identification in some CT images.

FIG 5. Contrast-enhanced CT scan of a feline thorax at the level of the eighth thoracic vertebra (cat 5); lung window, sternal recumbency. A caudodorsally located bronchioloalveolar mass occupies two-thirds of the left caudal lung lobe. The right caudal lung lobe and the accessory lobe are enlarged, but the lobar artery, bronchus and vein of the right caudal lung lobe are in a normal location. 8th = Eighth thoracic vertebra, BAC mass = Bronchial adenocarcinoma, acl = Accessory lung lobe, rcd = Right caudal lung lobe, v b a = Lobar vein, bronchus and artery

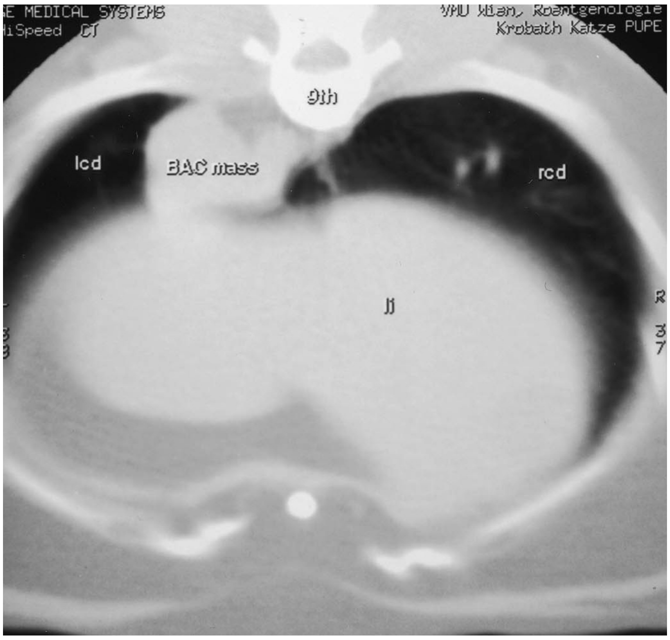

FIG 6. Contrast-enhanced CT scan of a feline thorax at the level of the ninth thoracic vertebra (cat 5); lung window, sternal recumbency. The lobar artery, bronchus and vein of the right caudal lung lobe are readily visible, whereas they are involved within the bronchioloalveolar mass on the left side which extends into the diaphragmatic recess further caudally. 9th = Ninth thoracic vertebra, BAC mass = Bronchial adenocarcinoma, lcd = Left caudal lung lobe, rcd = Right caudal lung lobe, li = Liver

Mediastinum – vessels and lymph nodes

All mediastinal vessels could be individually identified in most of the plain scans, and in every case after intravenous contrast injection. The cranial vena cava was the largest vessel, at 5 to 6 mm in diameter, followed by the brachiocephalic trunk (2 to 3 mm diameter) and the left and right subclavian artery (1·5 mm diameter) within the cranial mediastinum. The thoracic internal artery leaves the brachiocephalic trunk at the level of T1, and here also the thoracic internal vein enters the brachiocephalic vein (cats 1 and 3). Both brachiocephalic veins of 3 to 4 mm in size were visible until the level of T2 in cat 1. The caudal vena cava was identified in every case as a 5 to 8 mm thick vessel in the caudal mediastinum, either on the plain or contrast-enhanced scans. The descending aorta, measuring 4 to 5 mm in size, was always visible in the left caudodorsal mediastinum. The right azygos vein, of 1 mm in diameter, appeared right paravertebrally.

In the cranial mediastinum, displacement of all vessels to the right occurred in cat 3 due to right lung collapse. Dorsal displacement of the descending aorta, ventral displacement of the caudal vena cava, and left-sided displacement of the right azygos vein due to a large pulmonary mass were seen in cat 4 (Fig 1). Marked displacement of the decending aorta to the right paravertebral costal arch was found in cat 3 due to midline shift and overinflation of the left lung. The right azygos vein remained in place, but the descending aorta was situated to the right of it.

The mediastinal lymph nodes located at the second or third sternebrae could not be identified because they were not enlarged in any of the cats. The bronchial lymph nodes along the right side of the lung hilus were found to be enlarged in cat 3 and bilateral enlargement was found in the other four cats. Lymph node enlargement caused an increase in soft tissue around the left and right main stem bronchus. It did not cause narrowing of the lumen of the bifurcation or the main bronchi, except in cat 3.

Mediastinum – heart and pericardium

The heart, in the mid-mediastinum, was clearly identifiable in every case. After administration of the contrast medium, the atria and chambers of the heart became readily visible annd allowed a rough estimation of chamber wall thickness. Enlargement of the right ventricle was seen in cat 1; the lumen of the right atrium and the right ventricle were surrounded by a thin (1·5 to 2 mm) soft tissue layer representing the right and cranial walls of the heart. The lumen of the left ventricle was surrounded by a 5 to 8 mm thick muscular wall and its papillary muscles were clearly seen. Dorsal to the left ventricle was the left atrium, which was 10 to 12 mm in height and spanned nearly the whole base of the heart. The left atrium was seen to be about 5 mm in diameter to the left of the pulmonary trunk and lateroventral to the left main pulmonary artery. The heart was reduced in size in cat 3 and additionally displaced towards the right thoracic wall. General enlargement seen on the CT images in cats 2, 4 and 5 was confirmed on postmortem examination.

The aortic arch appeared as an oval-shaped, perpendicular-orientated structure. When scanning in a craniocaudal direction, it was always seen first, before the heart itself was imaged. The ascending aorta was about 6 mm in diameter and clearly identifiable because of hypodense fatty tissue around the base of the aortic origin. Dorsal to this section, the dividing pulmonary trunk was always seen. It showed a very short left main pulmonary artery of 3 to 4 mm in diameter, and accompanied the descending aorta on the left. The right main pulmonary artery appeared as a long bent vessel of the same size as the left pulmonary artery and was orientated to the right, crossing the base of the heart ventral to the tracheal bifurcation. The right main pulmonary artery separated immediately at the hilus into a cranial and caudal branch.

The pericardium was not visible in any cat.

Lungs

In the soft tissue (pleural) window, the normal air-filled lungs appeared totally hypodense (black) on plain scans. On contrast-enhanced scans, the now hyperdense vessels could be identified as bright spots within a black background. Only in the special lung window could the dividing bronchi and vessels be seen, producing a symmetrical pattern in the left and right lungs. Each lobe showed a main bronchus flanked by the artery laterally and the vein medially (Figs 2 to 6). The diameters of all these structures decreased from the hilus to the periphery, where they were unable to be individually identified and appeared as a reticular pattern of vascular and bronchial structures.

Evaluation of diseased lungs was performed using both the pleural and the lung window. In the pleural window, loss of air could be detected as a homogeneous or heterogeneous increase in soft tissue opacity or as a circumscribed encapsulated hyperdensity. Contrast administration enhanced the heterogeneity of the pattern. In cat 1, the right middle lobe appeared homogeneous (like liver), as a result of the total loss of normal vascular/bronchial reticular pattern and loss of air-filled alveoli, and remaining air was seen within large holes of ectatic bronchi producing a cavitary pattern (Fig 7). Generalised uptake of contrast medium into the diseased lobe was seen, with density increasing from about +40 to +90 HU. In cat 2, the caudodorsal part of the right caudal lobe appeared rather homogeneous and hyperdense, without visible bronchi. The fact that the study was performed postmortem, led to a generalised increase in density of the entire lung pattern due to loss of pulmonary air, resulting in a generalised ground-glass appearance (Fig 8).

Another general homogeneous opacity resulted from total loss of air in the whole right lung of cat 3 due to an enhancing mass which obstructed the main right bronchus. The bronchi were not visible, and the lung appeared atelectatic and

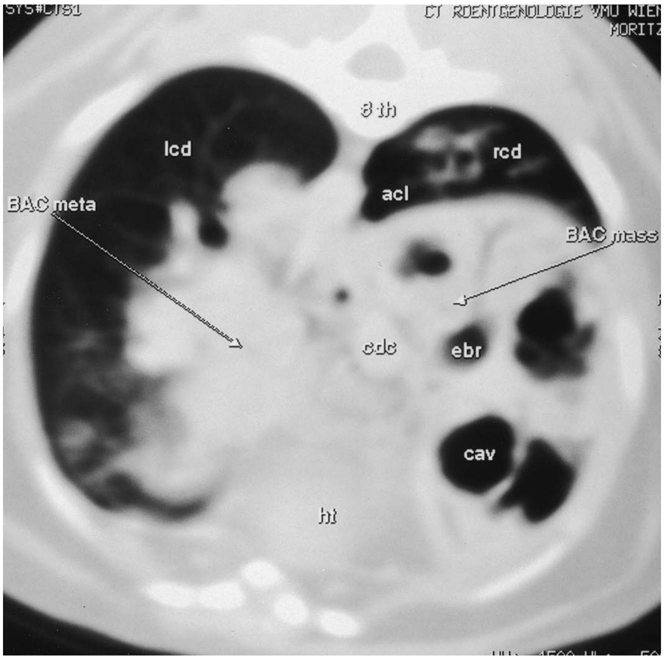

FIG 7. Contrast-enhanced CT scan of a feline thorax at the level of the eighth thoracic vertebra (cat 1); lung window, sternal recumbency. The bronchioloalveolar mass affects the right middle lung lobe and shows a 'hepatic' appearance, with enlarged bronchi and cavernous formations. It invades the mediastinum and also affects the left caudal lung lobe. The accessory lobe and right caudal lobe are displaced caudodorsally. 8th = Eighth thoracic vertebra, acl = Accessory lung lobe, rcd = Right caudal lung lobe, BAC mass = Bronchial adenocarcinoma, cdc = Caudal vena cava, ebr = Ectatic bronchus, cav = Cavitary lesion, ht = Heart, BAC meta = Metastatic bronchial adenocarcinoma, lcd = Left caudal lung lobe

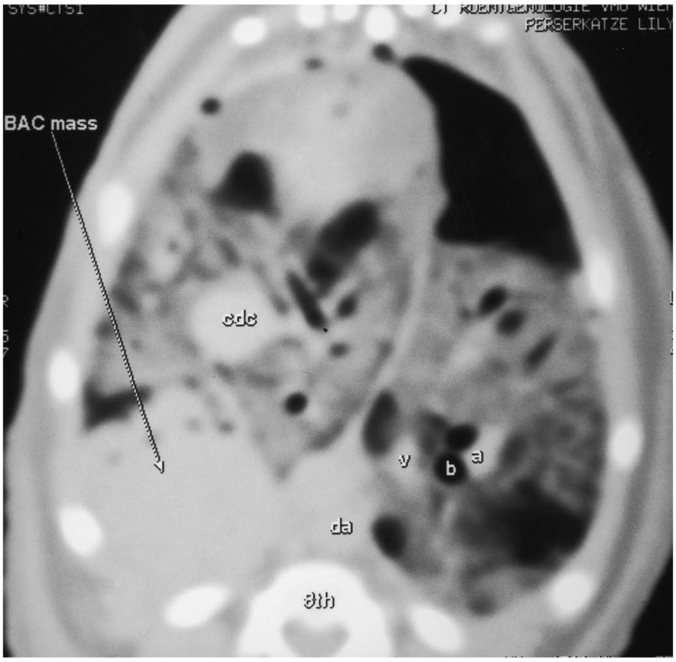

FIG 8. Plain CT scan of a feline thorax at the level of the eighth thoracic vertebra (cat 2, postmortem); lung window, dorsal recumbency. The bronchioloalveolar mass occupies the dorsal part of the right caudal lung lobe and is poorly defined against the 'normal' lung tissue which appears hyperdense due to partial postmortem atelectasis. Accumulation of free air ventral to the left lung is a postmortem artefact. BAC mass = Bronchial adenocarcinoma, 8th = Eighth thoracic vertebra, da = Descending aorta, v b a = Lobar vein, bronchus and artery of the left caudal lung lobe, cdc = Caudal vena cava

hyperdense after contrast administration. Diagnosis of lung atelectasis due to a right bronchial neoplastic mass could be made in cat 3. All right lung lobes were without any sign of air and no individual lobe could be identified. The left lung lobes appeared overinflated and there was mediastinal shift (Fig 9). The left hilar area appeared normal but the middle part and the periphery of the left main lobe were without any reticular pattern and showed marked signs of emphysema.

In cats 4 and 5, the caudodorsal pulmonary mass affected both lung and mediastinum and had invaded the diaphragmatic recess . After contrast medium administration, the CT pattern in cat 4 appeared more homogeneous with a slight rim enhancement, compared to cat 5. In the latter case, a more mixed CT pattern, showing hyperdense neoplastic tissue and focal non-enhancing areas within the mass, could be seen after contrast administration. The masses extended into the caudal mediastinum, merging with the oesophagus and/or displacing the descending aorta and caudal vena cava. It was impossible to determine the direction of the suspected neoplastic extension, even after contrast administration.

Measurement of Hounsfield units for tissue differentiation

Being a technique whereby tissue voxel attenuation coefficients are represented as image pixels, CT allows determination of the density of both normal and abnormal tissue. The density of normal lungs was found to decrease from cranial to caudal and from ventral to dorsal; values of –630 to –800 HU were found in plain scans, and were only slightly increased in contrast studies (–610 to –780 HU). Densities of diseased tissues in HU, along with brief imaging details, are given in Table 1.

CT-guided percutaneous fine needle aspiration biopsy

In cats 1, 3, 4 and 5, CT-guided percutaneous fine needle aspiration biopsy was performed, using a 20 gauge, 0·9×70 mm Luer-Lock Sterican hypodermic needle (Braun). The target lesion was evaluated using plain and contrast-enhanced CT with reference to the following criteria: location; association with a rib; connect-ion via thickened pleura to the thoracic wall; presence of neighbouring delicate structures such as heart, main vessels, bronchi, oesophagus or trachea; and density in HU corresponding to fluid or soft tissue. The main consideration was to avoid inducing a pneumothorax.

Each of the four cats remained in the same position as during the previous diagnostic CT. The proposed intercostal space for needle placement was first counted on the CT images and then repeated on the cat. The point of skin perforation was located, assisted by the horizontal and vertical plane of the laser light of the gantry. For a caudal lung mass, as in cat 4, a right paravertebral approach was used. Correct positioning of the needle was confirmed by a subsequent CT scan at the level of the target

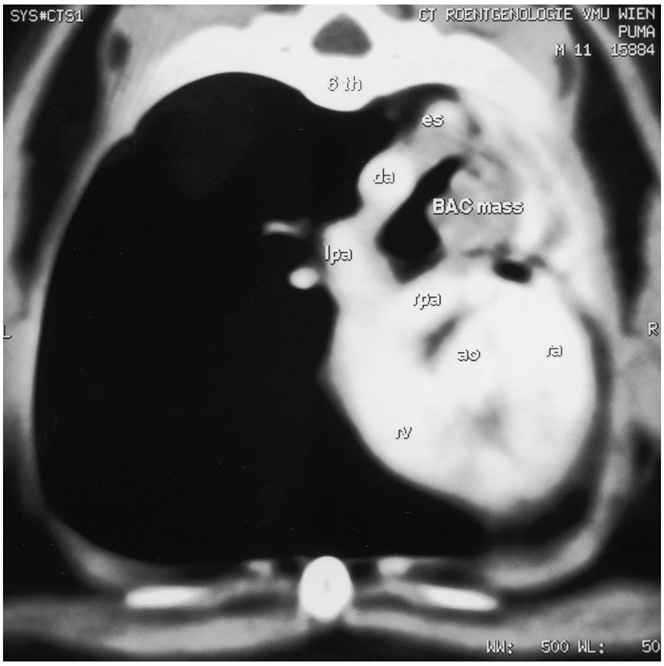

FIG 9. Contrast-enhanced CT scan of a feline thorax at the level of the sixth thoracic vertebra (cat 3); pleural window, sternal recumbency. A space-occupying bronchioloalveolar mass has led to the narrowing of the dividing bronchus and total atelectasis of the entire right lung. 6th = Sixth thoracic vertebra, es = Oesophagus, da = Descending aorta, BAC mass = Bronchial adenocarcinoma, lpa = Left pulmonary artery, rpa = Right pulmonary artery, ao = Aortic origin, ra = Right atrium, rv = Right ventricle

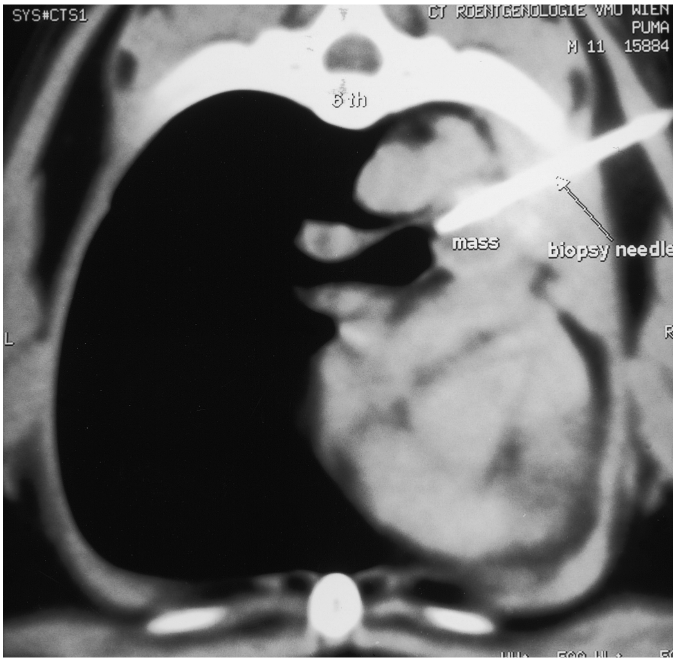

FIG 10. Contrast-enhanced CT scan of a feline thorax at the level of the sixth thoracic vertebra (cat 3); pleural window, sternal recumbency. This image shows CT-guided biopsy of a bronchioloalveolar mass; the tip of the needle lies slightly eccentric and near the lumen of the bronchus. 6th = Sixth thoracic vertebra, mass = Bronchial adenocarcinoma

lesion (Fig 10). Then aspiration was performed and repeated two or three times (see Table 1).

Cytology results indicated inflammation in case 1, although this was finally revealed to be adenocarcinoma of the right middle lung lobe following surgery. Bronchioloalveolar neoplasia was suspected as a result of fine needle aspiration biopsy in cats 3 and 5 and was confirmed as bronchial adenocarcinoma histopathologically. Cat 4 appeared to have some sort of pulmonary carcinoma after biopsy, which was finally diagnosed as a metastasis of a previously removed colonic carcinoma.

Haemoptysis, a well recognised complication of fine needle aspiration biopsy, was encountered in cat 3 during extubation. Anaesthesia was maintained to stop bleeding after a short period of increased-pressure ventilation.

DISCUSSION

The use of CT in the feline thorax has been rarely described, although the CT anatomy of the thorax in the cat has been established (Samii and others 1998). Clinical use of the technique has been demonstrated in one cat, in which CT-guided percutaneous biopsy was performed (Tidwell and Johnson 1994). In this case, the lung was punctured successfully to diagnose granuloma. No further descriptions of the CT pattern of feline thoracic lesions have been found in the veterinary literature.

In this clinical study of four cats with bronchial adenocarcinoma and one cat with lung metastasis, the lung tissue changes had common features. First, all processes, except in one case, involved the right lung lobes. This is also reported in man and dogs, but in the cat both sides seem to be equally affected by primary tumours (Koblik 1986). Secondly, all lung lobe opacities were associated with the main bronchi which were partially or totally obstructed. Thirdly, unilateral or bilateral lymph node enlargement and invasion of the mediastinum was seen. Fourthly, the loss of air within the lungs led to various different patterns of opacity. There was a rather heterogeneous opacity which consisted of soft tissue isodensity and hypodense areas suggestive of necrosis or mucoid detritus. This diseased lung tissue enhanced after contrast administration due to increased uptake of contrast medium in a sort of capsule. Hounsfield units increased from +21 to +72 in the plain image and up to +56 to +120 after intravenous injection in cats 1, 3, 4 and 5.

There were several differential diagnoses for the diseased lungs in these cats, including granulomatous lesion, pulmonary abscess, primary lung tumour, metastatic lung tumour, pneumonia, congenital cyst or parasitic lesion (Koblik 1986, Tilley and Smith 1997). All these processes will affect the lymph nodes and involve the mediastinum (Koblik 1986). Adenocarcinomas are found frequently in small animals, accounting for 70 to 80 per cent of pulmonary carcinomas, followed by squamous cell carcinoma and anaplastic carcinomas (Hawkins 1995). Adenocarcinomas may appear radiographically as focal, solitary, well-circumscribed masses, as localised consolidations or as multiple, poorly circumscribed masses (Koblik 1986). Bronchial carcinoma was considered in each of these cases because of the more solitary lesions involving main stem bronchi or lobar bronchi, invading the mediastinum, affecting the lymph nodes, and crossing the borders into the opposite lung. In the case of bronchioloalveolar carcinoma or adenocarcinoma in man, the CT pattern may be homogeneous or heterogeneous depending on the number, size and grade of mucoid cysts building up the neoplastic lesion (Stern and Swensen 1996). Solitary bronchial adenocarcinoma in man shows a density of +80 to +180 HU and marked contrast enhancement. The higher levels of HU indicate microscopic soft tissue calcification (Wegener 1992), which was not seen in any of these cats. After contrast administration the atelectatic lung tissue enhances, leaving the neoplastic area in between hypodense (Wegener 1992). Similar to reports in man, this was noticed in cats 1, 3 and 5.

Thoracic CT examinations are very sensitive, as has been demonstrated, but specificity of the changes is low, even after iodine contrast administration. Biopsy is always needed to give a final diagnosis (Tidwell and Johnson 1994). In four cats (1, 3, 4 and 5), percutaneous CT-guided fine needle aspiration biopsies were obtained. Cytology reports corresponded well with CT findings in all four cases, as increased soft tissue density can be found with inflammation as well as with neoplastic lesions. Inflammation was diagnosed by fine needle aspiration biopsy in cat 1; there was necrotic tissue material mainly consisting of toxin-damaged granulocytes, but no bacteria were found. However, the underlying tumour was missed. In cats 3, 4 and 5, clusters of changed bronchial and pulmonary cells indicating neoplasia were diagnosed. Aspiration had been performed blindly in cat 3 a week before CT, without conclusive results. It is not possible to distinguish definitively between inflammation and neoplasia from the CT pattern (Spann and others 1998). In neoplastic lesions, islets of necrotic tissue often occur which would correspond to the heterogeneous CT appearance and to 'false negative' cytological reports. Histopathological findings diagnosed bronchial adenocarcinoma and lymph node metastases in cats 1, 2, 3 and 5. The CT pattern in the similarly changed lung lobe in cat 4 made a neoplastic lesion likely, and finally lung metastasis of colonic carcinoma was diagnosed.

Thoracic CT is furthermore an ideal technique to gather detailed information about cats which are to undergo surgery (Spann and others 1998). Lung lobe resection of suspected pneumonia was successfully carried out on the basis of CT examination, as demonstrated in cat 1. However, the owner requested that the cat was euthanased after he found out the final diagnosis of bronchial adenocarcinoma.

In human medicine, special CT scan protocols and film interpretation courses are available (Wegener 1992, Kuhlman 1998, Padhani and Fishman 1998). In the veterinary literature, no standardisation for clinical use was found. On the basis of this study, the following film examination protocol for CT images of the feline thorax is proposed. Interpretation of the images starts with the thoracic spine, the ribs, the sternum and the muscular thoracic wall, followed by the pleural space and the area of the diaphragm. Next the mediastinum is evaluated, with careful examination of the trachea, oesophagus, vessels, lymph nodes, thymus gland and the heart. Finally, the bronchi and lungs are investigated. The advantage of this systematic approach is that it allows the clinician not simply to concentrate on obvious pathologies, but to take note of subtle changes which might influence therapy or prognosis. A structured approach to diagnostic reading is likewise adopted by radiologists in the interpretation of thoracic radiographs (Suter 1984, Thrall 1994).

Ideally, CT scanning of the thorax should be performed with the shortest possible exposure time and the animal should remain motionless at maximal inspiration (Burk 1991). This is virtually impossible to achieve, however, because the scan time usually is two to five seconds in third and fourth generation scanners, especially in the second-hand machines most likely to be encountered in the veterinary field. Creating a state of maximum motionless inspiration during a two second x-ray tube rotation for image aquisition is a huge challenge for the anaesthetist. Every image will be blurred due to motion artefacts of the thoracic wall. Hyperventilation is a method which has been described for intrathoracic biopsy technique (Tidwell and Johnson 1994). However, a major disadvantage is the increased loss of carbon dioxide which may result in respiratory alkalosis (Senior 1995). To overcome this unsatisfactory situation the present author has used the short expiratory pause to improve image quality (Henninger and Pavlicek 2001); an expiratory pause lasts about three seconds at a breathing rate of 12 breaths per minute. Incremental CT usually needs three to five seconds per scan. In a fast scan technique, two seconds per tube rotation is sufficiently short to go between two breaths. Ventilating the feline patient at its normal breathing rate after administration of a muscular relaxant proved to be satisfactory and tolerable for the anaesthetist (Auer 1998) and fulfils the considerations for radiation safety.

Acknowledgements
The author thanks Mag Dieter Malleczek and Dr Sibylle Kneissl from the Radiology Clinic, UVW, for the CT scanning. Dr Michael Leschnik and Dr Nicole Luckschander from the I. Medical Clinic for Small Animals and Horses, UVW, Dr Martina Mosing from the Central Anaesthesiology and Intensive Care Unit, UVW, and Dr Norbert Kopf from Small Animal Clinic Breitensee are also thanked for their contributions and for referring the feline patients.

References

AHLBERG, N-E., HOPPE, F., KELTER, U. & SVENSSON, L. (1989) A computed tomographic study of volume and x-ray attenuation of the lungs of beagles in various body positions. *Veterinary Radiology* **26**, 43-47

ASSHEUER, J. & SAGER, M. (1997) MRI and CT Atlas of the Dog. Blackwell, Berlin. pp 83-181

AUER, U. (1998) Anästhesie bei der thoraxchirurgie. Proceedings of the Weichteilchirurgie bei Hund und Katze. 13. VÖK-Jahrestagung, September 19-20, Innsbruck. pp 99-106

BURK, R. L. (1991) Computed tomography of thoracic diseases in dogs. *Journal of the American Veterinary Medical Association* **199**, 617-621

CHEN, Q., KLEIN, J. S., GAMSU, G. & WEBB, W. R. (1992) High-resolution computed tomography of the mammalian lung. *American Journal of Veterinary Research* **53**, 1218-1224

DELISLE, F. (1993) La tomodensitométrie des médicine vétérinaire. *Point Vétérinaire* **25**, 552-559

FARROW, C. S., GREEN, R. & SHIVELY, M. (1994) Radiology of the Cat. Mosby, St. Louis. pp 45-130

HATHCOCK, J. T. & STICKLE, R. L. (1993) Principles and concepts of computed tomography. *Veterinary Clinics of North America: Small Animal Practice* **23**, 399-416

HAWKINS, E. C. (1995) Diseases of the lower respiratory system. In: Textbook of Veterinary Internal Medicine, Vol 1. Eds S. J. Ettinger and E. C. Feldman. W. B. Saunders, Philadelphia. pp 792-809

HENNINGER, W. (1997) Computer- und resonanztomographie. Klinische indikationen bei haustieren. In: Handlexikon der Tierärztlichen Praxis, Lieferung 201. Ed E. Wiesner. Enke, Stuttgart. pp 161j-161zj

HENNINGER, W. & GUTMANNSBAUER, B. (1999) CT-anatomy of the canine mediastinum. In: Proceedings of the 5th EAVDI meeting 1998, Balsta, Sweden. *Veterinary Radiology and Ultrasound* **40**, 191

HENNINGER, W. & PAVLICEK, M. (2001) Konventionelle CT-untersuchungsprotokolle, erstellt nach regionen, für den optimalen kontrastmitteleinsatz beim hund. *Kleintierpraxis* **46**, 685-698, 761-772

KOBLIK, P. D. (1986) Radiographic appearance of primary lung tumors in cats. A review of 41 cases. *Veterinary Radiology* **27**, 66-73

KUHLMAN, J. E. (1998) Spiral CT: Thoracic applications. In: Spiral-CT. Techniques and Basic Principles. Eds E. K. Fishman and R. B. Jeffrey Jr. Lippincott-Raven, Philadelphia. pp 71-94

PADHANI, A. R. & FISHMAN, E. K. (1998) Spiral CT of lung cancer. In: Spiral-CT. Techniques and Basic Principles. Eds E. K. Fishman and R. B. Jeffrey Jr. Lippincott-Raven, Philadelphia. pp 95-114

SAMII, V. F., BILLER, D. S. & KOBLIK, P. D. (1998) Normal gross anatomy of the feline thorax and abdomen: comparison of computed tomography and cadaver anatomy. *Veterinary Radiology and Ultrasound* **39**, 504-511

SCHWARZ, L. A. & TIDWELL, A. S. (1999) Alternative imaging of the lung. *Clinical Techniques in Small Animal Practice* **14**, 187-206

SENIOR, D. F. (1995) Fluid therapy, electrolytes, and acid-base control. In: Textbook of Veterinary Internal Medicine, Vol 1. Eds S. J. Ettinger and E. C. Feldman. W. B. Saunders, Philadelphia. pp 305-312

SPANN, D. R., SELLON, R. K., THRALL, D. E., BOSTIAN, A. E. & BOSTON, G. T. (1998) Computed tomographic diagnosis: use of computed tomography to distinguish a pulmonary mass from alveolar disease. *Veterinary Radiology and Ultrasound* **39**, 532-535

STERN, E. J. & SWENSEN, S. J. (1996) High Resolution CT of the Chest. Comprehensive Atlas. Lippincott-Raven, Philadelphia. pp 181-189

SUTER, P. F. (1984) A Text Atlas of Thoracic Diseases of the Dog and Cat. Wettswil, Switzerland. pp 253-293, 517-734

THRALL, D. E. (1994) The mediastinum. In: Textbook of Veterinary Diagnostic Radiology, 3rd edn. Ed D. E. Thrall. W. B. Saunders, Philadelphia. pp 309-321

TIDWELL, A. S. & JOHNSON, K. L. (1994) Computed tomographic-guided percutaneous biopsy in the dog and cat: Description of technique and preliminary evaluation in 14 patients. *Veterinary Radiology and Ultrasound* **35**, 445-456

TILLEY, L. P. & SMITH Jr., F. W. K. (1997) The 5 Minute Veterinary Consult – Canine and Feline. Williams & Wilkins, Baltimore. p 324

WEGENER, O. H. (1992) Ganzkörpercomputertomographie, 2nd edn. Blackwell, Berlin. pp 135-242

ZOOK, B. C., HITZELBERG, R. A. & BRADLEY, E. W. (1989) Cross-sectional anatomy of the Beagle thorax. *Veterinary Radiology* **30**, 277-281